

Localization in the quantum Hall regime

Bernhard Kramer^{a,1}, Stefan Kettmann^a and Tomi Ohtsuki^b

^a *I. Institut für Theoretische Physik, Universität Hamburg, Jungiusstraße 9, 20355 Hamburg, Germany*

^b *Department of Physics, Sophia University, Kioicho 7-1, Tokyo 102-8554, Japan*

Abstract

The localization properties of electron states in the quantum Hall regime are reviewed. The random Landau model, the random matrix model, the tight-binding Peierls model, and the network model of Chalker and Coddington are introduced. Descriptions in terms of equivalent tight-binding Hamiltonians, and the 2D Dirac model, are outlined. Evidences for the universal critical behavior of the localization length are summarized. A short review of the supersymmetric critical field theory is provided. The interplay between edge states and bulk localization properties is investigated. For a system with finite width and with short-range randomness, a sudden breakdown of the two-point conductance from ne^2/h to 0 (n integer) is predicted if the localization length exceeds the distance between the edges.

Key words: quantum Hall effect, localization, network model, conductance distribution, Anderson transition

PACS: 74.40.Xy, 71.63.Hk

1. Introduction

The scaling theory of localization [1,2] predicts that there is no Anderson transition (AT) in two dimensions (2D) without interactions. There are only two known exceptions: One is the quantum Hall transition (QHT), and the other is the localization-delocalization transition in systems with spin-orbit interaction that are called the symplectic class. The former has attracted broad attention after the discovery of the quantum Hall effect (QHE) by Klaus von Klitzing in 1980 [3]. The symplectic class has been a subject of continuous effort with a strong increase after the discovery of the 2D metal-insulator transition (MIT) in Si-MOS-systems

[4] which also renewed the interest in whether or not Coulomb interaction can introduce an MIT in 2D.

In this paper, we mainly review results for the QHT. It has been noted immediately after its discovery that the QHE cannot be explained within the semiclassical Drude model which gives for the longitudinal conductivity $\sigma_{xx} = 0$ in the limit of large magnetic field, while the Hall conductivity $\sigma_{xy} = \nu e^2/h$. If the filling factor $\nu \equiv \rho h/eB$ is integer (ρ electron density), σ_{xy} is quantized in units of e^2/h . For explaining the QHE, a certain amount of disorder is necessary in order to understand why broad plateaus in the Hall conductivity can be formed and simultaneously the longitudinal conductivity drops to zero: localized states in the tails of the disorder broadened Landau bands can pin the Fermi level, but do not contribute to the transport. However, since there is a non-vanishing Hall conductivity, not all of the states can be localized. Near

¹ Corresponding author. E-mail: kramer@physnet.uni-hamburg.de

the centers of the Landau bands, regions of extended states must exist that can carry the Hall current [5]. That this current has the correct magnitude for giving integer values of the Hall plateaus first has been suggested by Prange [6] who showed that the amount of current which is lost when a localized state is formed in the tail of a Landau band is exactly compensated for by the remaining extended states. Later this has been argued to be related to a gauge property which was used to conjecture that if an equilibrium current is flowing in a quantum Hall system this can only give integer values of the Hall conductance [7,8]. For such an equilibrium current to flow, at least one extended state must exist. Thus the localization-delocalization phenomenon is closely related to the very existence of the Hall plateaus.

When introducing the standard models we concentrate predominantly on the aspect of universality of the transition. We argue that Coulomb interaction do not change the universality class of the QHT, apart from spin-orbit interaction which is still a subject of intense ongoing research. We mention in passing that the scaling properties of the QHT are also the subject of considerable experimental efforts. So far, temperature and frequency scalings of the conductances in the region of the QHE are fully consistent with the picture developed by the theory [9,10,11,12,13,14]. Furthermore, starting from the standard Chalker-Coddington network model we report on a class of equivalent Hamiltonians such as the Dirac model in which the QHT is associated with a crossover from zero to a finite non-zero mass.

Finally, recent results for the interplay between localization of bulk and edge states in systems of finite width are described. It is shown for short range impurities that if the localization length becomes equal to the system width, there can be an abrupt breakdown of the two-point quantum Hall conductance from the plateau value to zero. This is driven by a dimensional crossover between 2D and 1D localization of the bulk states resulting in an abrupt chiral metal to insulator transition of the edge states. It resembles a first order quantum phase transition.

2. The standard models

2.1. The random Landau model

The most straightforward description of the quantum Hall phenomena is obtained by adding a random potential $V(\mathbf{r})$ to the Hamiltonian of a free electron moving in a plane in the presence of a perpendicular magnetic field B ,

$$H = H_0 + V := \frac{1}{2m^*} (\mathbf{p} + e\mathbf{A})^2 + V(\mathbf{r}), \quad (1)$$

and solving the corresponding Schrödinger equation. In the Landau gauge, the vector potential is $\mathbf{A} = B(-y, x, 0)$; m^* and e are the effective mass of the electron and the elementary charge, respectively, and \mathbf{p} the momentum operator. The randomness is incorporated by assuming a distribution function for the potential. In the presence of spatial correlations,

$$\langle V(\mathbf{r})V(\mathbf{r}') \rangle = W^2 f(\mathbf{r} - \mathbf{r}') \quad (2)$$

where $\langle \dots \rangle$ denotes the configurational average. For simplicity, one often also assumes a symmetric potential distribution such that $\langle V(\mathbf{r}) \rangle = 0$. If the potential is white noise, $f(\mathbf{x}) = \delta(\mathbf{x})$. The correlator $f(\mathbf{x})$ reflects the nature and the range of the impurity potential.

In the representation of the Landau states $|nX\rangle$, $H_0|nX\rangle = E_n|nX\rangle$, the above Hamiltonian is

$$H = \sum_{nX} E_n |nX\rangle \langle nX| + \sum_{nX, n'X'} V_{nX, n'X'} |nX\rangle \langle n'X'| \quad (3)$$

with the matrix elements of the random potential, $V_{nX, n'X'}$, and the Landau energies $E_n = \hbar\omega_B(n + 1/2)$ ($n = 0, 1, 2, \dots$) that are degenerate with respect to the quantum number $X \equiv 2\pi m\ell_B^2/L_y$ ("center-of-motion coordinate", m integer) with a degree of $n_B = 1/2\pi\ell_B^2$ per unit area. Here, $\omega_B = eB/m^*$ and $2\pi\ell_B^2 = \hbar/eB$ are the cyclotron frequency and the cyclotron area, respectively. The degeneracy corresponds to the density of the flux quanta h/e in the system. For sufficiently large B the disorder induced coupling between the Landau levels can be neglected.

In this limit, the density of states $\rho(E)$ of a single band can be obtained exactly [15,16]. It is symmetric around the Landau band center and has Gaussian tails for $|E - E_n| \gg \Gamma$. Near the band center, one obtains $\rho(E) = \rho_n [1 - (E - E_n)^2/\Gamma^2]$. For the lowest band, $\rho_0 = n_B/\pi\Gamma$ and the band width $\Gamma = 2Wn_B^{1/2}$.

Using the Lifshitz argument [17], it can be argued that the wave functions are localized within accidentally formed potentials wells in the band tails. Towards the band centers, the localization length increases. Using the above Hamiltonian and with a random superposition of impurity potentials for modeling the randomness, first quantitative results for the localization in the lowest Landau bands have been obtained [18]. It was found that the exponential localization length ξ diverges near the centers of the Landau levels according to power laws

$$\xi(E) = \xi_n |E - E_n|^{-\nu_n}. \quad (4)$$

In the lowest Landau band, an exponent $\nu_0 \approx 2$ has been found. Figure 1 shows qualitatively the behavior of the density of states and the localization length.

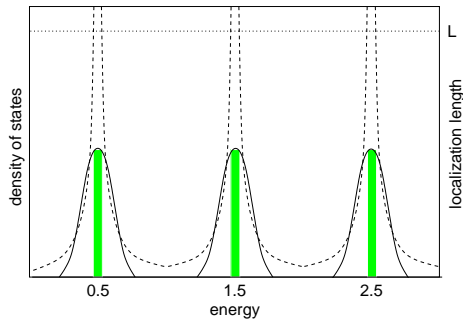


Fig. 1. Qualitative picture of the density of states (solid line) and the localization length (dashed) of the random Landau model (arbitrary units) as a function of the energy (units $\hbar\omega_B$). In the energy regions where the localization length exceeds a cutoff length L the wave functions are effectively delocalized (green regions of the density of states).

2.2. The random matrix model

Instead of calculating the matrix elements of the random potential from a superposition of impurity potentials, one can equivalently start from (3) and choosing the matrix elements of the potential according to their statistical properties [19]. If one is interested only in universal features the precise form of the matrix elements should not make any difference. The resulting Hamiltonian corresponds to a random matrix model. However, in contrast to the conventional random matrix Hamiltonians, the one derived from the Landau

Hamiltonian (1) has strongly correlated matrix elements. For the lowest Landau band and a Gaussian correlator (2) with correlation length $\sqrt{2}\sigma$

$$\langle V_{XX'} V_{X''X'''} \rangle = \delta_{X-X', X''-X'''} \frac{W^2 \ell_B}{\sqrt{2\pi} \beta L_\infty} \times \exp \left\{ -\frac{1}{2} \left[\beta^2 (X - X')^2 + \frac{1}{\beta^2} (X - X''')^2 \right] \right\} \quad (5)$$

with the parameter $\beta^2 := 1 + (\sigma/\ell_B)^2$ representing the correlation of the potential matrix elements along diagonals $X - X' = \text{const}$ and L_∞ the size of the system. Even if the starting point is completely uncorrelated white noise, $\sigma = 0$, the correlations in the matrix elements persist, $\beta = 1$.

From numerical evidence, one can conclude that these correlations are responsible for the singular behavior of the localization length in the centers of the Landau bands [20]. Mathematically, the properties of this class of correlated random matrix models have not yet been explored. This might provide valuable insights into the statistics of spectral properties like the level statistics and their critical behavior. Eventually, such an investigation of the properties of correlated banded matrices also might give insight into the generic mathematical structure behind the phenomenon of the QHT.

Very careful quantitative determinations of the critical exponent of such Hamiltonians have been carried out [21] by using the numerical scaling method introduced earlier [22,23,24,25]. The results are described in detail in [26]. It was found that the value of the exponent is universally $\nu = 2.35 \pm 0.03$ which is clearly different from the value 2.73 ± 0.02 for the 2D symplectic case [27]. This is up to now considered as the most reliable value which is remarkably close to an earlier non-rigorous suggestion $\nu = 7/3$ [28] which was obtained on the basis of a semiclassical percolation model augmented by a quantum tunneling argument (see below). In the lowest and the second lowest band for white noise potential and finite correlation length the same exponent was obtained within the numerical uncertainty (Fig. 2). Furthermore, the exponent also turned out to be independent of long range correlations in the impurity potential (see below). Thus, to the best of our knowledge, the QHT represents a quantum phase transition for which it has been possible within the numerical uncertainties explicitly to demonstrate universality

over a wide range of parameters for the first time.

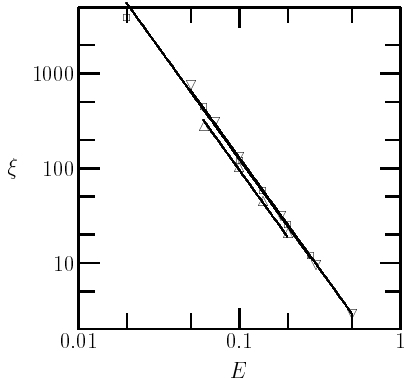


Fig. 2. Localization length ξ (units ℓ_B) as a function of the energy E (units Γ) for $n = 0$, $\sigma = 0$ (∇); $n = 0$, $\sigma = \ell_B$ (Δ); $n = 1$, $\sigma = \ell_B$ (\square) (from [29]).

2.3. The Peierls model

One of the standard models of localization is the Anderson Hamiltonian for a disordered system

$$H = \sum_j \epsilon_j |j\rangle\langle j| + \sum_{[jk]} V_{jk} |j\rangle\langle k|. \quad (6)$$

Here, j denote the sites of a hypercubic lattice, $\sum_j |j\rangle\langle j| = 1$ are the complete set of corresponding site states, ϵ_j the random site energies distributed randomly and independently in the interval $[-W/2, W/2]$, and V_{jk} the (real) hopping matrix elements between nearest neighbors that are in the simplest case assumed to be a constant V . This model often has been used in numerical studies of the localization problem in d dimensions without magnetic field [2]. In 2D, without disorder, the energy spectrum covers the range $-4V < E < 4V$. With disorder, the region of eigenenergies is $-4V - W/2 < E < 4V + W/2$, and all states are localized.

With magnetic field, the hopping matrix elements acquire Peierls phase factors [30,31]

$$V_{jk} = V \exp \left\{ -\frac{ie}{\hbar} \int_j^k \mathbf{dr} \cdot \mathbf{A}(\mathbf{r}) \right\} := V e^{i\alpha_{jk}}. \quad (7)$$

In the absence of disorder, the energy spectrum shows very rich and nontrivial self-similarity features that depend on the commensurability between the length scale imposed by the magnetic field and the lattice constant

a . This is the "Hofstadter butterfly" [32]. If the number of flux quanta per unit cell, $n_B a^2 := \alpha$ is rational, $\alpha = p/q$, the spectrum consists of q absolutely continuous bands of eigenenergies. If α is irrational, the spectrum is singularly continuous, it consists of a dense distribution of isolated eigenvalues. It can be shown by using the effective mass approximation that the spectrum becomes Landau like near the band edges.

Using the Peierls tight binding model, numerical studies showed delocalization in the centers of the bands [33] and quantization of the Hall conductivity in the localized regime [34].

2.4. The random network model

The origin of the randomness in a quantum Hall sample is mainly the random potential induced by the impurities in the bulk of the semiconductor sample due to the doping. In AlGaAs heterostructures the inversion layer is far from the doping layer. Therefore, the potential landscape seen by the electrons is rather smooth. Spatial correlations can be expected to be important when aiming at describing experimental results. Also from the theoretical viewpoint it turns out to be very useful to consider spatially long-ranged randomness. This is related to the fact that if the potential is smooth on the length scale of the magnetic field the eigenvalue problem can be discussed in terms of semiclassical approximation and the determination of the eigenstates becomes equivalent to a percolation problem [35,36,37,38,39,40].

If the correlation length of the random potential is large as compared to the magnetic length, $\sigma \gg \ell_B$, it can be shown that the dynamics of the electrons are governed by two totally different lengths scales. This limit can always be achieved if the magnetic field is assumed to be sufficiently large. In this limit, the eigenenergies are given by the equipotential lines,

$$E = \left(n + \frac{1}{2} \right) \hbar \omega_B + V(X, Y), \quad (8)$$

with center coordinates (X, Y) . The corresponding wave functions represent a slow drift of probability along the equipotential lines (length scale σ) of electrons that perform rapid cyclotron motions around (X, Y) (length scale ℓ_B). The direction of the probability current is perpendicular to the magnetic field and perpendicular to the local electric field represented by

the gradient of the potential along the equipotential line. Reversing the direction of the magnetic field reverses the direction of the current. Formally, the wave functions can be considered as waves superposed of the Landau states associated with the equipotential lines. The extension of the wave functions perpendicular to the equipotential lines is of the order of ℓ_B . Formally, one can approximate [40]

$$\psi(u, v) = C(u)\chi(v)e^{i\phi(u, v)} \quad (9)$$

with u and v the coordinates parallel and perpendicular to the equipotential line, respectively, $C^{-2}(u)$ the local electric field at $(u, v = 0)$ and $\phi(u, v)$ a gauge dependent phase. In this semiclassical limit, the allowed energies are determined from the condition that $\phi(u, v)$ must change by an integer multiple of 2π when moving around a closed equipotential contour.

The average total spatial extend of a given wave function is determined by the mean diameter of the randomly percolating equipotential line. When at some point the distance between two equipotential lines gets closer than ℓ_B , quantum tunneling will lead to coupling between corresponding wave functions. These regions correspond to saddle points of the potential. They are especially important near the center of the band (Fig. 3) where the critical behavior of the localization properties is expected to be determined by the competition between quantum interference and tunneling.

The percolation picture allows immediately to draw two important conclusions. First, at energies far away from the band center, corresponding to states in the tails of the band, the equipotential lines are closed percolating trajectories. Here, the wave functions are localized. Moving the energy towards the center of the band from above or below will increase the mean diameter of the percolating equipotential line. At some critical energy E_c near the band center, the equipotential line will percolate throughout the whole system (Fig. 3). This is the percolation threshold. For a symmetric potential distribution, this happens exactly at the band center. Thus, there is at least one energy, where the "classical" localization length — the mean diameter of the percolating cluster — becomes of the order of the size of the system. Second, according to percolation theory, the mean diameter of a connected cluster near the threshold diverges according to a power law, $\xi_p \propto |E - E_c|^{-\nu_p}$ [41], with the percolation critical exponent $\nu_p = 4/3$ [42,43]. It has been suggested [28]

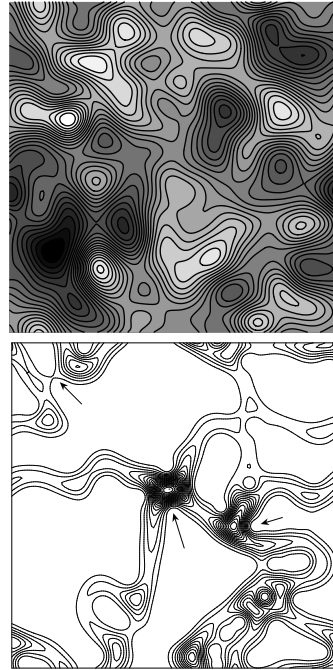


Fig. 3. Top: gray scale picture of a correlated random potential, $\sigma = 2\ell_B$, with equipotential lines, white: high, black: low potential; bottom: modulus of a wave function corresponding to an energy near the center of the Landau band extending essentially along equipotential lines, occasionally inter-connected via tunneling near the saddle points of the potential (arrows).

that tunneling across the saddle points supports the delocalization near the percolation threshold. In particular, it was argued that the localization exponent is increased exactly by 1, $\gamma = \nu_p + 1 = 7/3$.

Besides estimating the critical exponent, the semiclassical limit provides the background of a standard model for the physics of a system in the quantum Hall regime near the quantum critical point [44]. Basically, one replaces the irregular assembly of different saddle points of the semiclassical percolation network (Fig. 3) by a regular network of saddle point scatterers connected by links which carry the scattering wave functions associated with the above equipotential lines far away from a saddle point (Fig. 4).

Each saddle point has attached four links carrying amplitudes $\psi_1 \dots \psi_4$, two of them, say ψ_1, ψ_3 , describing incoming waves and the other two outgoing waves. As a result of the magnetic field incoming and outgoing waves are spatially separated, in contrast to a normal

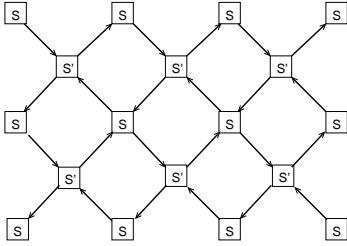


Fig. 4. Bipartite network of saddle points S, S' connected by links (after [44]). Directions of the probability currents in the links are indicated by arrows. Current directions change from clockwise to counter clockwise between neighboring loops in the diagonals.

transmission problem. By solving the scattering problem for a saddle point $V(x, y) = E_0 - ax^2 + by^2$ exactly [45], the transmission probability at energy $\epsilon := (E - E_0)/\ell_B^2(ab)^{1/2}$ was found, $|t|^2 = 1/[1 + \exp(-\pi\epsilon)]$.

In terms of the reflection and transmission amplitudes, r and t , respectively, the scattering properties of the saddle point can be parametrized as

$$\begin{pmatrix} \psi_2 \\ \psi_4 \end{pmatrix} = \mathbf{S} \begin{pmatrix} \psi_1 \\ \psi_3 \end{pmatrix} \quad (10)$$

with the scattering matrix

$$\mathbf{S} = \begin{pmatrix} e^{-i\phi_2} & 0 \\ 0 & e^{i\phi_4} \end{pmatrix} \begin{pmatrix} -r & t \\ t & r \end{pmatrix} \begin{pmatrix} e^{i\phi_1} & 0 \\ 0 & e^{-i\phi_3} \end{pmatrix} \quad (11)$$

with $|r|^2 + |t|^2 = 1$. The phases ϕ_j ($j = 1 \dots 4$) correspond to the waves in the links. At \mathbf{S}' (Fig. 4), the role of incident and outgoing channels is interchanged.

Exactly at the energy of the saddle point, $r(E_0) = t(E_0) = 1/\sqrt{2}$. If $E \ll E_0$, $r \approx 1$, and the incoming waves ψ_1, ψ_2 are completely reflected into outgoing waves ψ_2, ψ_4 , respectively. If $E \gg E_0$, $t \approx 1$. In this case, ψ_1, ψ_2 are transmitted into ψ_4, ψ_2 , respectively. These latter energy regions correspond to wave functions localized completely within the loops of the network — equivalent to the valleys and the mountains of the potential landscape — while in the former case the wave functions can extend across the whole network.

By numerically calculating the transmission through a network of identical saddle points but with random phases in the links, the critical behaviour of the localization length has been determined. The critical exponent in the lowest Landau band was found to be consistent with the values obtained earlier [44].

In order to better understand the critical point, the real-space renormalization group approach has been adapted to describe the critical point of the Chalker-Coddington network model [46,47,48,49]. The results obtained for the exponent are in good agreement with the earlier findings. In summary, it appears now that there is more than convincing evidence for the picture of the QHT as a universal quantum phase transition. In the next section, we provide an overview of the experimental evidences that this quantum phase transition is indeed physically realized in the QHE experiments.

2.5. The Dirac model

The above network model of Chalker and Coddington is defined in terms of a scattering problem *at a given energy*. This is of great practical usefulness for studying the localization critical behaviour. By reconstructing from the transfer matrix the underlying Hamiltonian one can arrive at a class of models that allows to relate the QHT to other quantum critical phenomena.

First, we establish a connection between the network model with a *tight binding model*. We re-arrange the network in the way shown in Fig. 5. The loops that are inter-connected by the saddle points are arranged as a 2D lattice such that the centres of the loops are associated with lattice points $\mathbf{R}_{xy} = x\mathbf{e}_x + y\mathbf{e}_y$ with integer x, y and $x + y = \text{even}$. The x - and y -directions are assumed parallel to the directions of the links that connect S and S' (Fig. 4). The links between adjacent saddle points within each of the loops (denoted by arrowheads labelled with $\lambda = 1, \dots, 4$ in Fig. 5 [50]) are associated with four "site" states. These are then characterized by the lattice vector and the "quantum number" λ . They are assumed to form a complete set and are connected within a given unit cell and between nearest neighboring cells via tunneling across the saddle points.

The matrix elements of the effective Hamiltonian can be determined following [50,51]. The vector of the amplitudes at \mathbf{R}_{xy} after $M + 1$ iterations is

$$\psi_{\mathbf{R}\lambda}(M + 1) = \sum_{\mathbf{R}'\lambda'=1}^4 U_{\mathbf{R}\lambda, \mathbf{R}'\lambda'} \psi_{\mathbf{R}'\lambda'}(M). \quad (12)$$

The unitary operator \mathbf{U} describes the evolution of the wave function between M and $M + 1$. The eigenstates of the $4L$ -dimensional matrix \mathbf{U} (L system size)

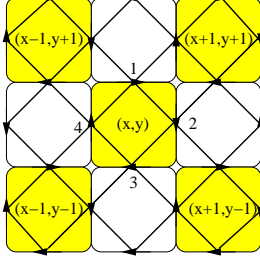


Fig. 5. The network model re-arranged as a tight binding model on a 2D square lattice with four basis states per "site" (grey squares) at position (x, y) ($x + y = \text{even}$). The links between the saddle points in Fig. 4 (indicated here by \diamond) are associated with the basis states (arrowheads). They are connected by tunneling (thick solid lines) across the saddle points.

$$\mathbf{U} |\psi_\alpha\rangle = e^{i\omega_\alpha(E)} |\psi_\alpha\rangle \quad (\alpha = 1 \dots 4L) \quad (13)$$

with eigenvalues 1 ($\omega_\alpha(E) = 0$) are the stationary states of the network with an energy parametrized by the energy dependent reflection parameter of the saddle points, $r \equiv r(E) = \sqrt{1 - t^2(E)}$.

Interpretation of (12) as a "time dependent" Schrödinger equation, $\psi(M+1) - \psi(M) = (\mathbf{U} - \mathbf{1})\psi(M)$, suggests to relate \mathbf{U} to a self-adjoint Hamiltonian \mathbf{H} ,

$$\mathbf{H} := \frac{1}{2i} (\mathbf{U}^\dagger - \mathbf{U}), \quad (14)$$

with quasi-energy eigenvalues $\epsilon_\alpha = \hbar\omega_\alpha(E)$.

Since each lattice point is connected via four saddle points to its nearest neighbors, \mathbf{U} has a 4×4 block structure. Due to the bipartite structure of the links each of the 4×4 blocks has a 2×2 block structure. By suitably arranging amplitudes one gets

$$\mathbf{U} = \begin{pmatrix} 0 & \mathbf{M} \\ \mathbf{N} & 0 \end{pmatrix} \quad (15)$$

which gives for the effective Hamiltonian

$$\mathbf{H} = \frac{1}{2i} \begin{pmatrix} 0 & \mathbf{N}^\dagger - \mathbf{M} \\ \mathbf{M}^\dagger - \mathbf{N} & 0 \end{pmatrix}. \quad (16)$$

The matrices

$$\mathbf{M} = \begin{pmatrix} te^{i\phi_1} \tau_-^x \tau_+^y & re^{i\phi_1} \\ re^{i\phi_3} & -te^{i\phi_3} \tau_+^x \tau_-^y \end{pmatrix}, \quad (17)$$

$$\mathbf{N} = \begin{pmatrix} re^{i\phi_2} & te^{i\phi_2} \tau_+^x \tau_+^y \\ te^{i\phi_4} \tau_-^x \tau_-^y & -re^{i\phi_4} \end{pmatrix}, \quad (18)$$

are obtained using the scattering matrix \mathbf{S} . They contain translation operators τ_\pm connecting neighboring cells

$$\tau_\pm^x \psi_{\mathbf{R}\lambda} = \psi_{\mathbf{R} \pm \mathbf{e}_x \lambda} \quad \tau_\pm^y \psi_{\mathbf{R}\lambda} = \psi_{\mathbf{R} \pm \mathbf{e}_y \lambda}. \quad (19)$$

Inserting this into the Hamiltonian one notes that within a given cell, say at \mathbf{R} , the Hamiltonian matrix elements are proportional to the reflection amplitudes

$$h_{\mathbf{R}j, \mathbf{R}j-1} = \frac{ir}{2} e^{i\phi_j}, \quad (20)$$

with $j = 1, 2, 3, 4$ cyclic (such that $j-1 := 4$ for $j = 1$). The eight matrix elements that couple nearest neighbor cells contain the transmission amplitude t ,

$$h_{\mathbf{R}2, \mathbf{R}+3} = \frac{it}{2} e^{i\phi_2}, \quad h_{\mathbf{R}3, \mathbf{R}+4} = \frac{-it}{2} e^{i\phi_3}, \quad (21)$$

$$h_{\mathbf{R}4, \mathbf{R}-1} = \frac{it}{2} e^{i\phi_4}, \quad h_{\mathbf{R}1, \mathbf{R}+2} = \frac{it}{2} e^{i\phi_1}, \quad (22)$$

with $\mathbf{R}_{\pm\pm} := \mathbf{R} + (\pm 1, \pm 1)$ (Fig. 5). The remaining matrix elements are the conjugates of these.

When the phases ϕ_j are independent of the lattice point \mathbf{R} , and all of the saddle points are identical, the system is periodic. The Hamiltonian can be diagonalized exactly with a Bloch Ansatz

$$\psi_\lambda(\mathbf{R}) = e^{i\mathbf{q}\cdot\mathbf{R}} u_\lambda(\mathbf{q}). \quad (23)$$

The resulting band structure $\epsilon(\mathbf{q})$ can be straightforwardly obtained in a closed form. It consists of two bands separated by a gap Δ at $\mathbf{q} = 0$. This can be seen most easily by considering the eigenvalue problem for \mathbf{H}^2 instead of \mathbf{H} . Exactly at the energy of the (identical) saddle points, $r = t = 1/\sqrt{2}$ and the gap vanishes, $\Delta = 0$. For energies close to the saddle point, one expands $r := 1/\sqrt{2} + \Delta/4$ ($\Delta \ll 1$). One finds in this case $\Delta = 2\sqrt{(1-2rt)}$ when assuming $\sum_{j=1}^4 \phi_j = \Phi = \hbar\phi/e = h/2e$.

The formation of the gap can be understood in better detail by expanding the band structure near $\mathbf{q} \approx 0$. One finds for small Δ

$$\epsilon^2(\mathbf{q}) = \Delta^2 + (\mathbf{q} - e\mathbf{A})^2 \quad (24)$$

with a "vector potential" $\mathbf{A} = (1/2)(\phi_1 - \phi_3, \phi_4 - \phi_2)$. In this "effective mass approximation", one can show that the Hamiltonian has the Dirac form

$$\mathbf{H} = (p_x - eA_x)\sigma_x + (p_y - eA_y)\sigma_y + m\sigma_z + \phi\mathbf{1}, \quad (25)$$

with the components of the momentum operator $p_j = -\hbar i \partial_j$ ($j = x, y$), the mass $m \equiv \Delta$, and the Pauli matrices $\sigma_1, \sigma_2, \sigma_3$.

In this Hamiltonian, randomness can be introduced in different ways. Via randomness in the individual phases one can make the components of the vector potential random. Randomizing the total Aharonov-Bohm phases in the loops produces randomness in the "scalar potential" ϕ . Finally, assuming the tunneling parameters of the saddle points to be random gives fluctuations in the mass parameter m .

The correspondence between the quantum Hall problem, certain tight binding models, and the 2D Dirac model has been noted by several authors [52,53,54,55,56]. Fisher and Fradkin [52] have reached the Dirac model starting from a 2D tight binding model with diagonal on-site disorder in a perpendicular magnetic field with half a flux quantum per unit cell. They constructed a field theory for the diffusive modes which was shown to be in the same universality class as the orthogonal $O(2n, 2n)/O(2n) \times O(2n)$ ($n \rightarrow 0$) non-linear σ -model. This implies that all states are localized as in the absence of a magnetic field and suggests that if delocalization occurs with magnetic field, it must be a direct consequence of breaking time-reversal symmetry instead of some other property of the field. Generalizations to the several-channel scattering problem have also been discussed [53].

Ludwig and collaborators [54] have used a tight binding model on a square lattice with nearest and next-nearest neighbor coupling, half a flux quantum per unit cell and a staggered potential energy $\mu(-1)^{x+y}$ as a starting point. At low energy, this model was shown to be equivalent to a Dirac model with two Dirac fields. Without disorder the model exhibits an IQHE phase transition as a function of a control parameter which is essentially the mass m of the lighter Dirac field. The transition belongs to the 2D-Ising universality class. The associated exponents and the critical transport properties were determined. The density of states is

$$\rho(\epsilon) = \frac{|\epsilon|}{\pi} \Theta(\epsilon^2 - m^2). \quad (26)$$

It can readily be obtained from (25) with $\mathbf{A} = 0$. Applying linear response theory to the Dirac system one can determine the Hall conductivity by calculating the ratio of, say, the current density in the x -direction, j_x and the electric field, E_y , in the y -direction

$$\sigma_{xy} \equiv \frac{j_x}{E_y} = \frac{e^2}{h} \frac{m}{2\pi^2} \int \frac{d^2 q d\omega}{[(i\omega - \epsilon)^2 - q^2 - m^2]^2}. \quad (27)$$

It is found that at zero energy, $\epsilon = 0$, where the above density of states vanishes, the Hall conductivity jumps by e^2/h at $m = 0$ (Fig. 6)

$$\sigma_{xy}(m) = -\frac{\text{sgn}(m)}{2} \frac{e^2}{h}. \quad (28)$$

The heavier Dirac field contributes towards the Hall conductivity with $e^2/2h$ such that the total Hall conductivity jumps from 0 to e^2/h . Simultaneously, the magneto-conductivity σ_{xx} is non-zero,

$$\sigma_{xx} = \sigma_0 \frac{e^2}{h} \delta_{m,0}, \quad (29)$$

with the Kronecker-symbol $\delta_{m,0}$ equal to 1 for $m = 0$ and 0 for $m \neq 0$, and the constant σ_0 of the order $\pi/8$. The critical point shows time-reversal, particle-hole and parity invariance. Thus, the clean 2D Dirac

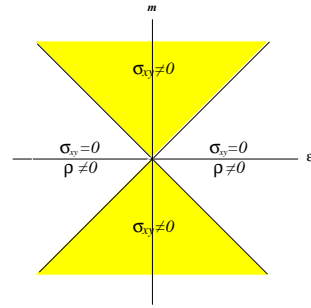


Fig. 6. The phase diagram of the ordered Dirac model [54] showing regions of non-zero density of states ρ ($|\epsilon| > |m|$) and non-zero Hall conductivity $\sigma_{xy} = \pm e^2/2h$ ($|\epsilon| < |m|$).

model exhibits a QHT at $\epsilon = m = 0$. By introducing randomness in the Dirac mass, $m = m(x, y)$, the wave functions are confined to the contours $m(x, y) = 0$. Then, the QHT can be interpreted in terms of quantum percolation of these states. In the absence of randomness of the phases (i.e. the vector potential), the corresponding critical exponent of the correlation length is that of the classical percolation model.

Introducing disorder in the various parameters of the model leads to breaking of the symmetries, as indicated in Table 1. Taking into account only randomness in the scalar potential, it was argued that the transition can be described by a symplectic non-linear sigma model.

The case of only a random vector potential can be treated to a large extent analytically [57,58,59,60,61] and it has many remarkable properties. The model exhibits a fixed line in this case. The zero-energy wave function was exactly determined. It was found to be

Table 1

Symmetry breaking by disorder in the various kinds of parameters of the Dirac model (\mathbf{p} momentum operator; m Dirac mass parameter; σ vector of the Pauli matrices $\sigma_x, \sigma_y, \sigma_z$; ϕ scalar potential; \mathbf{A} vector potential).

symmetry	$\sigma \cdot \mathbf{p}$	$m\sigma_z$	ϕ	$\sigma \cdot \mathbf{A}$
parity	yes	no	no	no
time reversal	yes	no	yes	no
particle-hole	yes	no	no	yes

extended and showed multifractal scaling. The density of states was found to show a power law dependence on the energy near $\epsilon \approx 0$ with the exponent varying continuously upon moving along the fixed line while the diagonal conductivity was found to be constant. With all three different types of disorders included, the Dirac model is equivalent to the Chalker-Coddington network model with randomness in the saddle points included.

3. One-parameter scaling

Table 2 contains a representative selection of exponents numerically obtained so far from numerical investigations done on different models. The question arises how the QHT, i.e its critical properties can be investigated experimentally.

3.1. The scaling picture

As the QHT is a quantum phenomenon in an *infinite* system at zero temperature, it is obvious that for determining the critical behavior some extrapolation method is required. This has been developed [23,24,25] by starting from the finite size scaling method previously established for conventional phase transitions [68].

One defines a quantity X which depends on a set of parameters x_i characterizing the system, such as the Fermi energy, the variance of the disorder, the magnetic field, and the system size L ,

$$X = f(\{x_i\}, L). \quad (30)$$

We assume the existence of a scaling law

$$X = F(\chi L^{1/\nu}, \phi_1 L^{y_1}, \phi_2 L^{y_2}, \dots), \quad (31)$$

Table 2

Selection of critical exponents in the lowest Landau band. Abbreviations: CCN (Chalker-Coddington network model), CNS (Chern number scaling), DLS (double layer system with white noise randomness), FRI (finite range impurities), PTB (Peierls tight binding Hamiltonian), RGF (recursive Green function method), RLM (random Landau matrix model), RSN (random saddle point network model), SSC (superspin chain) RSR (real space renormalization), SCD (self-consistent diagrammatic perturbation theory), SOS (spin orbit scattering), SRI (short range impurities), TNS (Thouless number scaling), TMS (transfer matrix scaling), FSS (finite size scaling)

exponent ν	model	method	reference
∞	SRI	SCD	[62]
≈ 2	PTB	TMS	[33]
≈ 2.0	SRI	RGF	[18]
2.35 ± 0.03	RLM	RGF	[21,26,27]
2.3 ± 0.08	RLM	RGF	[63]
2.4 ± 0.2	RLM	RGF	[29]
2.4 ± 0.1	FRI	CNS	[64]
≈ 2.3	SOS	TNS	[65]
≈ 2	DLS	TNS	[66]
2.5 ± 0.5	CCN	TMS	[44]
2.43 ± 0.18	RSN	TMS	[67]
2.5 ± 0.5	CCN	RSR	[46]
2.39 ± 0.01	CCN	RSR	[49]
2.38 ± 0.4	SSC	FSS	[80]

with χ being the relevant scaling variable and ϕ_i denote the irrelevant ones. The latter nevertheless can cause corrections to scaling as long as the system size is finite. In a numerical calculation they must not be ignored. These variables characterize distances from the critical point, $\nu > 0$ is the critical exponent and $y_i < 0$ are the irrelevant exponents. For large enough system size, only the relevant scaling variable survives, and (31) becomes

$$X = F_1\left(\frac{L}{\xi}\right), \quad (32)$$

with $\xi \sim \chi^{-\nu}$. The quantity χ as a function of some control parameter, say x , can be expanded near the critical point x_c

$$\chi = a_1(x - x_c) + a_2(x - x_c)^2 + \dots \quad (33)$$

For $L \rightarrow \infty$, the scaling variable X should show a singularity at the localization-delocalization critical point. Most conveniently, the localization lengths $\lambda(L; x) < \infty$ of a quasi-1D system can be used, with L the cross sectional system diameter [23]. Consider now

$$\Lambda(L; x) := \frac{\lambda(L; x)}{L}. \quad (34)$$

For parameters such that $\Lambda(L \rightarrow \infty; x) \rightarrow 0$ the system is localized with the localization length $\xi(x) := \lambda(L \rightarrow \infty; x) < \infty$. If $\Lambda(L \rightarrow \infty; x) \rightarrow \infty$ the system is delocalized. Here, $\lambda^{-1}(L \rightarrow \infty; x)$ corresponds to the dc-conductivity [23,24]. The critical point is defined by $\Lambda(L \rightarrow \infty; x) := \Lambda_c = \text{const}$. Most efficiently, $\lambda(L; x)$ can be calculated using the transfer matrix method. The quasi-1D localization length is then given by the inverse of the smallest of the Lyapunov exponents of the transfer matrix [25].

Instead of the localization length one can also consider as scaling variables other physical quantities such as the conductance, the level statistics and the statistics of the wave functions. However, up to now the most precise determinations of the critical behavior have been achieved using the localization lengths (Tab. 2).

3.2. Experimental scaling

Guided by the above one-parameter scaling method, one can infer the behavior of the localization length from the scaling behavior of the experimentally determined conductivity components with temperature T , frequency ω or the geometrical size of the sample. In energy regions where the localization length exceeds some cutoff length L_c , the wave functions appear effectively as extended, and the longitudinal conductivity $\sigma_{xx} \neq 0$. In the localized regions, $\xi(E) < L$, $\sigma_{xx} \rightarrow 0$ for $T \rightarrow 0$. Correspondingly, in the latter regions $\sigma_{xy} = \text{const}$ while in the former σ_{xy} shows steps between successive Hall plateaus. The widths of the conductivity peaks and/or the width of the steps in the Hall conductivity reflect the widths of the energy regions of the effectively extended wave functions.

The cutoff length can have very different physical origins. For system size $L \rightarrow \infty$, at finite temperature, phase breaking processes, as for instance induced by electron-phonon or electron-electron scattering, lead to a temperature dependent phase breaking length $L_\phi(T) \propto T^{-p/2}$. Similarly, for finite frequency

$\omega \neq 0$, the phase breaking length is $L_\omega \propto \omega^{-z}$. On the other hand, for $T \rightarrow 0$ and $\omega \rightarrow 0$, it is eventually the geometrical size of the system which plays the role of the cutoff. In summary,

$$L_c = \min(L_\phi, L_\omega, L). \quad (35)$$

For instance, the temperature dependence of the peaks in the dc-conductivity component σ_{xx} and the width of the corresponding steps in σ_{xy} can then be estimated starting from the idea that the peak width is related to the width of the energy interval $\Delta(T) := 2E_c(T)$ of the effectively extended states determined by the condition $L_\phi(T) = \xi(E_c) \propto |E_c|^{-\nu}$. This yields $\Delta(T) \propto T^{p/2\nu} := T^\kappa$ [9]. Such a behavior has indeed been found in many experiments with a non-universal exponent $\kappa = 0.42$ [9,10,11]. An extensive description of the data collected until 1995, and their interpretation, is given in [26]. Recent measurements including the frequency scaling [12,13,14] confirm the scaling picture.

Thus, to the best of our knowledge one can state that the QHE is indeed a manifestation at finite T of a universal quantum phase transition at $T = 0$.

4. The quest for the critical theory

The numerical and experimental evidence for the universality of the quantum Hall transition raises expectations that a full characterization of this quantum critical point will result in the analytical derivation of its critical exponents and the scaling functions. Soon after the discovery of the QHE a field theory has been derived from the microscopic Hamiltonian of the random Landau model (1) [70], and (3) [71,72]. It was shown to have two coupling parameters σ_{xx}^0 and σ_{xy}^0 , the longitudinal and Hall conductance as defined on small length scales of the order of the elastic mean free path l . This field theory is based on the theory of localization of electrons in weakly disordered systems.

In order to describe localisation, one needs to go beyond perturbation theory in the disordered potential, and has to take full advantage of the symmetries arising in the calculation of correlation functions of disordered systems. This complication can be traced back to the fact that the disorder averaged electron wave function amplitude $\langle \psi(\mathbf{x}, t) \rangle$ decays on length scales on the order of l , and contains no information on localisation. Rather, in order to capture quantum localisation, one

needs to consider higher moments of the wave function amplitudes, such as the impurity averaged evolution of the electron density $n(\mathbf{x}, t) = \langle |\psi(\mathbf{x}, t)|^2 \rangle$. Thus, in a more formal language, a nonperturbative averaging of products of retarded and advanced propagators, $\langle G^R(E)G^A(E') \rangle$ is needed to obtain information on quantum localisation.

In a useful analogy to the study of spin systems, the field theoretical approach contracts the information on localisation into a theory of Goldstone modes Q , arising from the global symmetry of rotations between the functional integral representation of the retarded propagator G^R ("spin up") and the advanced propagator G^A ("spin down"). The field theory can either be formulated by means of the replica trick, where the N replicas can be represented either by N fermionic or N bosonic fields, yielding a bounded or unbounded symmetric space, respectively, on which the modes Q are defined [70].

Because of the necessity and the difficulty to perform the limit $N \rightarrow 0$ at the end of the calculation a more rigorous supersymmetric field theory has been formulated. This technique represents the product of Green functions $G^R(E)G^A(E')$ by functional integrals over two fermionic and bosonic field components, composing a supersymmetric field vector ψ . The supersymmetric representation enables one to perform the averaging over the disorder potential as a simple Gaussian integral [71,72].

As a result of the averaging one obtains an interacting theory of the fields ψ containing an interaction term $\propto \psi^4$, where the *interaction strength* is proportional to the variance of the disorder potential W^2 (2). This term can now be decoupled by introducing another Gaussian integral over Q -matrices. Clearly, the field Q should not be a scalar, otherwise we would simply reintroduce the Gaussian integral over the random potential V . Rather, in order to be able to describe the physics of localization, the field Q should capture the full symmetry of the functional integral representation of the correlation function. Therefore, the Gaussian integral is chosen to be over a 4×4 matrix Q which itself is an element of the symmetric space defined by the matrices A that leave the functional integral invariant under the transformation $\psi \rightarrow A\psi$. In the supersymmetric formulation, this matrix consists of two blocks of 2×2 matrices whose parameter space consists of a compact (bounded) and a noncompact (unbounded) sector. The

off-diagonal blocks, so to say the rotations between the compact and the noncompact sector, are then found to be parametrised by Grassmann (fermionic) variables.

Correlation functions such as the electron density and the conductivity can then be obtained from a partition function of these fields Q . The spatial variations of Q are governed by the action

$$S[Q] = \frac{\pi\hbar}{4\Delta\tau} \int \frac{d\mathbf{x}}{L^2} \text{Tr} Q^2(\mathbf{x}) + \frac{1}{2} \int d\mathbf{x} \langle \mathbf{x} | \text{Tr} \ln G(\hat{x}, \hat{p}) | \mathbf{x} \rangle \quad (36)$$

where

$$G^{-1}(\hat{x}, \hat{p}) = \left[\frac{(\omega + i\delta)\Lambda_3}{2} - \frac{(\hat{p} - qA)^2}{2m^*} - V_0(\hat{x}) + \frac{i\hbar}{2\tau} Q(\hat{x}) \right] \quad (37)$$

where $1/\tau$ is the elastic scattering rate, and Δ the mean level spacing related to the variance of the disorder potential (2) according to $W^2 = \Delta\hbar/2\pi\tau$. The 4×4 matrix Λ_3 is the diagonal Pauli matrix in the sub-basis of the retarded and advanced propagators, $\delta > 0$ and $\omega = E - E'$ break the symmetry between the retarded and advanced sector.

It turns out that the physics of diffusion and localisation, which arises on length scales much larger than the elastic mean free path l , is governed by the action of the long wavelength modes of Q . Thus, one can simplify and proceed with the analysis by expanding around a homogeneous solution of the saddle point equation, $\delta S = 0$. For $\omega = 0$, this is

$$Q = \frac{i}{\pi\nu} \langle \mathbf{x} | \left[E - H_0 - V_0(\mathbf{x}) + \frac{i}{2\tau} Q \right]^{-1} | \mathbf{x} \rangle. \quad (38)$$

This saddle point equation is solved by $Q_0 = \Lambda_3 P$, which corresponds to the self consistent Born approximation for the self energy of the impurity averaged Green function. At $\omega = 0$, rotations U which leave the action invariant yield the complete manifold of saddle point solutions as $Q = \bar{U}\Lambda_3 P U$, where $U\bar{U} = 1$.

The modes which leave Λ_3 invariant can be factorized out, leaving the saddle point solutions in this supersymmetric theory to be elements of the semi-simple supersymmetric space $Gl(2 | 2)/[Gl(1 | 1) \times Gl(1 | 1)]$ [72].

In addition to these gapless modes there are massive longitudinal modes with $Q^2 \neq 1$ which only change the

short distance physics, and not the physics of localization. They can be integrated out [70,71]. Thus, the partition function reduces to a functional integral over the transverse modes U .

The action at finite frequency ω and slow spatial fluctuations of Q around the saddle point solution can be found by an expansion of the action S . Inserting $Q = \bar{U}\Lambda_3 P U$ into (36) and performing the cyclic permutation of U under the trace Tr [70] allows a simple expansion to first order in the energy difference ω and to second order in the commutator $U[H_0, \bar{U}]$. The first order term in $U[H_0, \bar{U}]$ is proportional to the local current. It is found to be finite only at the edge of the wire in a strong magnetic field, due to the chiral edge currents. It can be rewritten as

$$S_{xyII} = -\frac{1}{8} \int d\mathbf{x} dy \frac{\sigma_{xy}^{0II}(\mathbf{x})}{e^2/h} \text{STr}(Q\partial_x Q\partial_y Q) \quad (39)$$

where the prefactor is the nondissipative term in the Hall conductivity in self consistent Born approximation [71]

$$\sigma_{xy}^{0II}(\mathbf{x}) = -\frac{1}{\pi} \frac{\hbar c^2}{m^2} \langle \mathbf{x} | (x\pi_y - y\pi_x) \text{Im} G_E^R | \mathbf{r} \rangle, \quad (40)$$

where $\pi = (\hbar/i)\nabla - q\mathbf{A}$. This field theory has now the advantage that one can treat the physics on different length scales separately: the physics of diffusion and localization is governed by the action of spatial variations of U on length scales larger than the mean free path l . That is why this field theory is often called diffusive nonlinear sigma model.

The physics on smaller length scales is included in the coupling parameters of the theory, which is identified in the above derivation as correlation functions of Green functions in self consistent Born approximation, being related to the conductivity by the Kubo-Greenwood formula,

$$\sigma_{\alpha\beta}^0(\omega, \mathbf{x}) = \frac{\hbar}{\pi L^2} \langle \mathbf{x} | \pi_\alpha G_{0E}^R \pi_\beta G_{0E+\omega}^A | \mathbf{x} \rangle. \quad (41)$$

The remaining averaged correlators, involve products $G_{0E}^R G_{0E+\omega}^R$ and $G_{0E}^A G_{0E+\omega}^A$ and are therefore by a factor $\hbar/\tau E$ smaller than the conductivity, and can be disregarded for small disorder. Using the Kubo formula (41), the action of Q simplifies to

$$S = \frac{\hbar}{16e^2} \int d\mathbf{x} \sum_{i=x,y} \sigma_{ii}^0(\omega=0, \mathbf{x}) \text{Tr} [(\nabla_i Q(\mathbf{x}))^2] - \frac{\hbar}{8e^2} \int d\mathbf{x} \sigma_{xy}^0(\omega=0, \mathbf{x}) \text{Tr} [Q\partial_x Q\partial_y Q] \quad (42)$$

where $\sigma_{xy}^0(\omega=0, \mathbf{x}) = \sigma_{xy}^I(\omega=0, \mathbf{x}) + \sigma_{xy}^{II}(\omega=0, \mathbf{x})$ and $\sigma_{xy}^I(\omega=0)$ is the dissipative part of the Hall conductivity in self consistent Born approximation (41).

The first term in this action yields localization in 2D electron systems, signaled by the presence of a gap in the field theory. The second term could not be obtained by any order in perturbation theory. It is of topological nature. In 2D and for a homogenous Hall conductance it can be shown that this term can take only discrete purely imaginary values,

$$S_{\text{Top}} = 2\pi i \frac{\hbar}{e^2} \sigma_{xy}^0 n, \quad (43)$$

where the integers n count how often the field $Q(\mathbf{x})$ is winding around its symmetric space as it varies spatially in 2D.

This theory was studied by means of a multi-instanton expansion, where one sums over all solutions with different topological numbers n , of the saddle point equation $\delta S = 0$, and integrates out fluctuations around these instanton solutions on length scales exceeding l . Thereby one finds that the conductance parameter σ_{xx}^0 becomes renormalized to smaller values, but that this renormalization flow towards localization is slowed down at half-integer values of the Hall conductance, $\sigma_{xy}^0 = (n + 1/2)e^2/h$. This derivation is valid at large conductance parameters σ_{xx}^0 . On this basis the two-parameter scaling of the quantum Hall transition has been suggested (Fig. 7) [70,73].

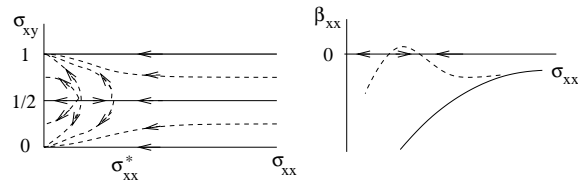


Fig. 7. The conjectured two parameter flow diagram of the integer quantum Hall effect (left), and the corresponding β -function, $\beta_{xx} = d \ln \sigma_{xx} / d \ln L$ (right) at $\sigma_{xy} = 1/2$ (dashed line) and at $\sigma_{xy} = 0$ (full line).

Subsequently, it has been shown rigourously that this field theory is indeed critical at half integer Hall conductance parameters σ_{xy}^0 [70,74,75], and that it has a spectral gap to fluctuations at other values of σ_{xy}^0 . This indicates the localization of the electron eigenstates of the random Landau model in the tails of the Landau bands [76]. Since the longitudinal conductance at the critical point σ^* is known to be smaller than 1,

the critical point is located in the strong coupling limit of the field theory. Thus, it is outside of the validity of available analytical methods which can be used to extract quantitative information on the critical exponents.

Recently, there has been nevertheless major progress, since it has been proven that the Hamiltonian of a chain of antiferromagnetically interacting superspins is equivalent to the nonlinear sigma model for short ranged disorder at $\sigma_{xy} = 1/2$ [77], as well as to the Chalker-Coddington model [78]. These proofs provide strong analytical support for the notion of universality of the QHT. This model of antiferromagnetically interacting superspins has been shown to be critical [79]. Numerically, the critical exponent ν was obtained from a finite length scaling of superspin chains to be $\nu = 2.38 \pm .4$ [80].

So far, no analytical information could be directly obtained on the critical parameters, the localization exponent ν and the critical value Λ_c of the scaling function. However, building on this model of a superspin chain, supersymmetric conformal field theories have been suggested, which ultimately should yield the critical parameters of the QHT [81,82].

Restricting this theory to quasi-1D, by assuming a finite width L_y of the quantum Hall bar, of the order of the unitary noncritical localisation length $\xi_{2Dunit} = l \exp(\pi^2 \sigma_{xx}^2)$, which serves as the ultraviolet cutoff of the conformal field theory, one finds that the critical value of the scaling function $\Lambda_c = 1.2$ (the ratio of the localisation length in a Quantum Hall wire and its finite width L_y , when the energy is in the center of the Landau band, see Section 3.1) is fixed by the eigenvalues of the Laplace-Beltrami operator of this supersymmetric conformal field theory [82,84]. This is a characteristic invariant of this theory, arising from the conformal symmetry (just as the quantisation of angular momentum arises from the rotational symmetry of a Hamiltonian). Furthermore, based on the properties of this constrained class of supersymmetric conformal field theories, it has been predicted that the distribution function of local wave function amplitudes is very broadly, namely log-normally, distributed. This prediction has recently been confirmed by high-accuracy numerical calculations [85].

The quest to derive the critical exponent of the localisation length at the QHT from a critical supersymmetric theory has thus recently gained much progress,

but is still not yet complete .

5. The mesoscopic quantum Hall transition

Until here, the localization-delocalization transition in infinite systems with periodic boundary conditions in one direction has been considered. Using this model, it has been shown that disorder removes the degeneracy of the Landau bands and introduces delocalized states only at one energy in each band.

If Dirichlet boundary conditions are used the degeneracy of the Landau levels is removed even without disorder due to the confining potential. The eigenenergies form bands $\epsilon_n(X)$ which start at the positions of the Landau levels and $\epsilon_n(X) \propto X^2$ for $X \gg L$. In the latter energy region, the wave functions are 1D objects. They are delocalized along the edges of the system. They have chiral character such that the corresponding probability currents propagate in opposite directions at opposite edges. In the perpendicular direction, the edge wave functions are sharply localized with a distance $\ll \ell_B$. It has been shown that the quantization of the Hall conductance can be understood in terms of these edge states [8]. Commonly, it is argued that disorder does not influence the edge states since forward and backward scattering are spatially separated.

However, numerical data indicate that this is not always true. For short-range disorder, edge and bulk-localized states can mix [86]. Then, several questions can be asked. For instance, can the extended wave functions near the centers of the Landau bands coexist with the edge states in the presence of disorder? If they don't, what are the localization properties of the mixed states? Where do the 1D delocalized edge states go if the confining potential is continuously depleted?

In order to study such questions, quantum Hall wires with a finite width have to be considered. This has been done previously with the emphasis on conductance fluctuations [87,88], edge state mixing [89,90,91,92,93,94,95] and the breakdown of the QHE [96]. It has been suggested that edge wave functions might become localized if in the presence of white noise disorder edge and bulk states mix [92,93,95].

That this is indeed the case has been shown recently analytically and numerically [97]. In particular, it has been demonstrated that for $T = 0$ the two-terminal

conductance and the Hall conductance of a quantum wire in a magnetic field exhibit discontinuous transitions between the integer plateau values and zero, for uncorrelated disorder and hard wall confinement, as shown in Fig. 8. This is shown to be caused by chiral-metal to insulator transitions of the quasi-1D edge states, driven by a crossover from 2D to 1D localization of the bulk states. These metal-insulator transitions resemble first-order phase transitions in the sense that the localization length abruptly jumps between exponentially large and finite values. In the thermodynamic limit *fixing the aspect ratio* $c = L/L_y$ *when sending* $L \rightarrow \infty$, and only then $c \rightarrow \infty$, the two terminal conductance jumps between exactly integer values and zero conductance. The transitions occur at energies where the localization length of the bulk states is equal to the geometrical wire width, and m edge states can mix. When this happens, the electrons are free to diffuse between the wire boundaries but become Anderson localized along the wire.

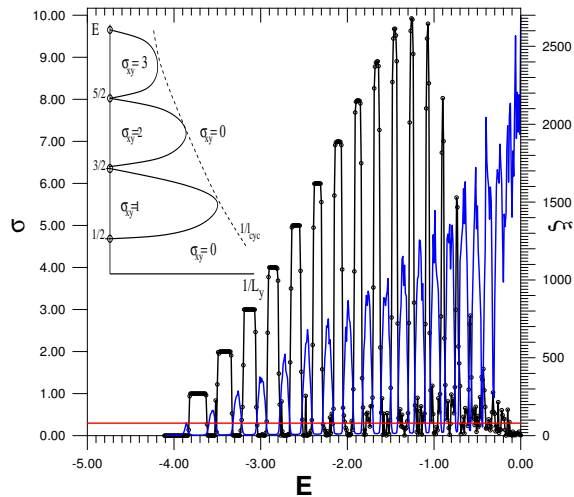


Fig. 8. Black curve (left scale): two-terminal conductance σ of a quantum Hall wire described by the Peierls tight binding model (lattice constant a) with Dirichlet boundary conditions (width $L_y = 80 a$, length $L = 5000 a$, disorder $W = 0.8 V$, magnetic field 0.025 flux quanta per unit cell) in units of e^2/h as a function of the energy E (units V). Blue curve (right scale): localization length $\xi(E)$ calculated with the transfer matrix method for a quantum wire with periodic boundary conditions ($L \leq 100000 a$); horizontal red line: $L_y = 80 a$. Inset: schematic phase diagram of the quantum Hall wire with $L \gg L_y$. Full lines: boundaries where σ_{xy} jumps from $m e^2/h$ to 0 (m integer, $L_y = \ell_{\text{cycl}}$, dotted).

6. Conclusion

In conclusion, we have reviewed the standard models of localization in the quantum Hall regime. We have provided an overview of the numerical results for the critical exponent of the localization length. The fact that these were obtained by using completely different models including white noise and long range correlated disorder strongly suggests that the QHT is a universal quantum phase transition. This also suggests that as long as interactions can be treated on a mean field level the critical exponent is not changed. Many experimental data indicate that the QHE is a manifestation of this quantum phenomenon. For quasi-1D quantum Hall systems, we have predicted that the mixing of bulk and edge states near the centers of the Landau levels leads to a crossover between 2D and 1D localization with drastic consequences for the conductance: the two-terminal conductance drops sharply from the plateau value to zero conductance at the energies where the bulk localization length is equal to the geometrical width of the system. This *mesoscopic quantum-Hall-insulator transition* should be observable in quantum wires with short range disorder.

Acknowledgement The authors would like to thank Prof. S. M. Nishigaki and PD Dr. B. Huckestein for useful discussions. We thank Bodo Huckestein for providing the original of Fig. 2. The work was supported by the Deutsche Forschungsgemeinschaft via the Priority Programme "Quanten-Hall-Systeme" (Project Kr627/10) and by the EU via grants FMRX-CT98-0180 and HPRN-CT2000-0144. The authors thank the Max Planck Institute for Physics of Complex Systems in Dresden for the hospitality during the completion of this article.

References

- [1] E. Abrahams, P.W. Anderson, D. C. Licciardello, and T.V. Ramakrishnan, Phys. Rev. Lett. **42**, 673 (1979).

- [2] B. Kramer, A. MacKinnon, Rep. Progr. Phys. **56**, 1469 (1993).
- [3] K. von Klitzing, G. Dorda, M. Pepper, Phys. Rev. Lett. **45**, 494 (1980).
- [4] S. V. Kravchenko *et al.*, Phys. Rev. B **51**, 7038 (1995).
- [5] H. Aoki, T. Ando, Sol. St. Commun. **18**, 1079 (1981).
- [6] R. E. Prange, Phys. Rev. B **23**, 4802 (1981).
- [7] R. B. Laughlin, Phys. Rev. B **23**, 5631 (1981).
- [8] B. I. Halperin, Phys. Rev. B **25**, 2185 (1982).
- [9] H. P. Wei, D. C. Tsui, M. A. Paalanen, and A. M. M. Pruisken, Phys. Rev. Lett. **61**, 1294 (1988).
- [10] S. Koch, R. J. Haug, K. v. Klitzing, and K. Ploog, Phys. Rev. Lett. **67**, 883 (1991).
- [11] L. W. Engel, *et al.*, D. Shahar, C. Kurdak, and D. C. Tsui, Phys. Rev. Lett. **71**, 2638 (1993).
- [12] F. Kuchar, R. Maisels, T. Brandes, B. Kramer, Europhys. Lett. **vv**, ppp (199y)
- [13] M. Furlan, Phys. Rev. B **57**, 14818 (1998).
- [14] F. Hohls, U. Zeitler, and R. J. Haug, Phys. Rev. Lett. **88**, 036802 (2002); F. Hohls *et al.*, Phys. Rev. Lett. **89**, 276801 (2002).
- [15] F. Wegner, Z. Phys. B **51**, 279 (1983).
- [16] E. Brézin, D. J. Gross, C. Itzykson, Nucl. Phys. B **235**[FS11], 24 (1984).
- [17] I. M. Lifshitz, Sov. Phys. Usp. **7**, 549 (1965).
- [18] T. Ando, H. Aoki, Phys. Rev. Lett. **54**, 832 (1985).
- [19] B. Huckestein, B. Kramer, Sol. St. Commun. **71**, 445 (1989).
- [20] M. Janssen, K. Pracz, Phys. Rev. B **61**, 6278 (2000).
- [21] B. Huckestein, B. Kramer, Phys. Rev. Lett. **64**, 1437 (1990).
- [22] A. MacKinnon, J. Phys. C: Sol. St. Phys. **13**, L1031 (1980).
- [23] A. MacKinnon, B. Kramer, Phys. Rev. Lett. **47**, 1546 (1981).
- [24] A. MacKinnon, B. Kramer, Z. Phys. B **53**, 1 (1983).
- [25] B. Kramer, A. MacKinnon, Rep. Progr. Phys. **56**, 1469 (1993).
- [26] B. Huckestein, Rev. Mod. Phys. **67**, 357 (1995).
- [27] Y. Asada, K. Slevin, T. Ohtsuki, Phys. Rev. Lett. **89**, 256601 (2002).
- [28] G. V. Mil'nikov, I. M. Sokolov, Pis'ma Zh. Eksp. Teor. Fiz. **48**, 494 [JETP Lett. **48**, 536 (1988)].
- [29] B. Huckestein, Europhys. Lett. **20**, 451 (1992).
- [30] R. Peierls, Z. Phys. **80**, 763 (1933).
- [31] J. M. Luttinger, Phys. Rev. B **84**, 814 (1951).
- [32] D. R. Hofstadter, Phys. Rev. B **14**, 2239 (1976).
- [33] L. Schweitzer, B. Kramer, A. MacKinnon, J. Phys. C **17**, 4111 (1984).
- [34] A. MacKinnon, B. Kramer, Z. Phys. B **vv**, ppp (1985).
- [35] M. Tsukada, J. Phys. Soc. Japan **41**, 1466 (1976).
- [36] S. V. Iordanski, Sol. St. Commun. **43**, 1 (1982).
- [37] R. F. Kazarinov, S. Luryi, Phys. Rev. B **25**, 7626 (1982).
- [38] Y. Ono, in: *Anderson Localization*, Springer Ser. Sol. State Sciences **39** (ed. by Y. Nagaoka, H. Fukuyama) p. 207 (Springer Verlag, Berlin 1982).
- [39] R. E. Prange, R. Joynt, Phys. Rev. B **25**, 2943 (1982).
- [40] S. A. Trugman, Phys. Rev. B **27**, 7539 (1983).
- [41] D. Stauffer, Phys. Rep. **54**, 2 (1979).
- [42] M. P. M. den Nijs, J. Phys. A **12**, 1857 (1979).
- [43] J. L. Black, V. J. Emery, Phys. Rev. B **23**, 429 (1981).
- [44] J. T. Chalker, P. D. Coddington, J. Phys. C **21**, 2665 (1988).
- [45] H. A. Fertig, Phys. Rev. B **38**, 996 (1988).
- [46] A. G. Galstyan, M. E. Raikh, Phys. Rev. B **56**, 1422 (1997).
- [47] D. P. Arovas, M. Janssen, B. Shapiro, Phys. Rev. B **56**, 4751 (1997).
- [48] M. Janssen, R. Merkt, J. Meyer, A. Weymer, Physica B **256-258**, 65 (1998).
- [49] P. Cain, R. A. Römer, M. Schreiber, M. E. Raikh, Phys. Rev. B **64**, 235326 (2001); R. A. Römer, P. Cain, Adv. Sol. St. Phys. **43**, 235 (Springer Verlag, Berlin 2003).
- [50] C. M. Ho, J. T. Chalker, Phys. Rev. B **54**, 8708 (1996).
- [51] R. Klesse, M. Metzler, Europhys. Lett. **32**, 229 (1995).
- [52] M. P. A. Fisher, E. Fradkin, Nucl. Phys. B **251**[FS13], 457 (1985).
- [53] E. Fradkin, Phys. Rev. B **33**, 3257 (1986); *ibid.* 3263.
- [54] A. W. Ludwig, M. P. A. Fisher, R. Shankar, G. Grinstein, Phys. Rev. B **50**, 7526 (1994).
- [55] D.-H. Lee, Phys. Rev. B **50**, 10788 (1994).
- [56] K. Ziegler, Europhys. Lett. **28**, 549 (1995).
- [57] Y. Aharonov, A. Casher, Phys. Rev. A **19**, 2461 (1979).
- [58] A. A. Nersesyan, A. M. Tselik, F. Wegner, Phys. Rev. Lett. **72**, 2628 (1994); NUcl. PHys. B **438**, 561 (1995).
- [59] D. Bernard, Nucl. Phys. B **441**, 471 (1995).
- [60] J.-S. Caux, I. I. Kogan, A. M. Tselik, Nucl. Phys. B **466**, 444 (1996).

- [61] I. I. Kogan, C. Mudry, A. M. Tselik, Phys. Rev. Lett. **77**, 707 (1996).
- [62] Y. Ono, J. Phys. Soc. Japan **51**, 2055 (1982).
- [63] B. Miek, Europhys. Lett. **13**, 453 (1990).
- [64] Y. Huo, R. Bhatt, Phys. Rev. Lett. **68**, 1375 (1992).
- [65] C. B. Hanna, D. P. Arovas, K. Mullen, S. M. Girvin, Phys. Rev. B **52**, 5221 (1995).
- [66] E. S. Sørensen, A. H. MacDonald, Phys. Rev. B **54**, 10675 (1996).
- [67] D.-H. Lee, Z. Wang, S. Kivelson, Phys. Rev. Lett. **70**, 4130 (1993).
- [68] M. N. Barber, in: *Phase Transitions and Critical Phenomena*, Vol **8**, ed. by C. Domb, J. Lebowitz (Academic London 1983), p. 146.
- [69] H. P. Wei, D. C. Tsui, M. A. Paalanen, A. M. M. Pruisken, Phys. Rev. Lett. **61**, 1294 (1988).
- [70] H. Levine, S. B. Libby, and A. M. M. Pruisken, Phys. Rev. Lett. **51**, 1915 (1983); Nucl. Phys. B **240** 30; 49; 71 (1984).
- [71] K. B. Efetov, *Supersymmetry in Disorder and Chaos* Cambridge University Press, Cambridge (1997).
- [72] H. A. Weidenmüller, Nucl. Phys. B **290**, 87 (1987); H. A. Weidenmueller and M. R. Zirnbauer, Nuclear Physics B **305**, 339 (1988).
- [73] D. E. Khmel'nitskii, JETP Lett. **38**, 552 (1983).
- [74] I. Affleck, Nucl. Phys. B **265**, 409 (1986).
- [75] S. Kettemann and A. Tselik, Phys. Rev. Lett. **82**, 3689 (1999).
- [76] K. B. Efetov, and V. G. Marikhin, Phys. Rev. B **40**, 12126 (1989).
- [77] M. R. Zirnbauer, Ann. d. Phys. **3**, 513 (1994).
- [78] D.H. Lee, Phys. Rev. B **50**, 10 788 (1994); J. Kondev and J.B. Marston, Nucl. Phys. B **497**, 639 (1997); M.R. Zirnbauer, J. Math. Phys. **38**, 2007 (1997).
- [79] J. B. Marston and Shan-Wen Tsai, Phys. Rev. Lett. **82**, 4906 (1999).
- [80] J. Kondev and J. B. Marston, Nuclear Physics B **497**, 639 (1997).
- [81] M. Zirnbauer, hep-th/9905054.
- [82] M.J. Bhaseen, I. I. Kogan, O. A. Soloviev, N. Taniguchi and A. M. Tselik, Nucl. Phys. B **580**, 688 (2000).
- [83] R. Klesse, M. R. Zirnbauer, Phys. Rev. Lett. **86**, 2094 (2001).
- [84] M. Janssen, M. Metzler, M. R. Zirnbauer Phys. Rev. B **59** 15836 (1999).
- [85] F. Evers, A. Mildemberger, and A.D. Mirlin, Phys. Rev. B **64**, 241303(R) (2001).
- [86] Y. Ono, T. Ohtsuki, B. Kramer, in: *High Magnetic Field in Semiconductor Physics*, ed. by G. Landwehr, Springer Ser. Sol. St. Sci. **101**, p. 60 (Springer, Berlin 1992).
- [87] G. Timp, A. M. Chang, P. Mankiewich, R. Behringer, J. E. Cunningham, T. Y. Chang, R. E. Howard, Phys. Rev. Lett. **59**, 732 (1987); G. Timp, R. Behringer, J. E. Cunningham, R. E. Howard, Phys. Rev. Lett. **63**, 2268 (1989).
- [88] T. Ando, Phys. Rev. B **49**, 4679 (1994).
- [89] B. J. van Wees, L. P. Kouwenhoven, E. M. M. Willems, C. J. P. M. Harmans, J. E. Mooij, H. van Houten, C. W. J. Beenakker, J. G. Williamson, C. T. Foxon, Phys. Rev. B **43**, 12431 (1991).
- [90] B. I. Shklovskii, Pis'ma Zh. Eksp. Teor. Fiz. **36**, 43 (1982) [JETP Lett. **36**, 51 (1982)]; A. V. Khaetskii and B. I. Shklovskii, Zh. Eksp. Teor. Fiz. **85**, 721 (1983) [Sov. Phys. JETP **58**, 421 (1983)].
- [91] M. E. Raikh, T. V. Shahbazyan, Phys. Rev. B **51**, 9682 (1995).
- [92] T. Ohtsuki, Y. Ono, Sol. St. Commun. **65**, 403 (1988); ibid. **68**, 787 (1988).
- [93] Y. Ono, T. Ohtsuki, B. Kramer, J. Phys. Soc. Jpn. **58**, 1705 (1989); T. Ohtsuki, Y. Ono, J. Phys. Soc. Jpn. **58**, 956 (1989).
- [94] T. Ando, Phys. Rev. B **42**, 5626 (1990).
- [95] R. G. Mani, K. v. Klitzing, Phys. Rev. B **46**, 9877 (1992); R. G. Mani, K. von Klitzing, K. Ploog, Phys. Rev. B **51**, 2584 (1995).
- [96] P. G. N. d. Vegvar, A. M. Chang, G. Timp, P. M. Mankiewich, J. E. Cunningham, R. Behringer, R. E. Howard, Phys. Rev. B **36**, 9366 (1987).
- [97] S. Kettemann, B. Kramer, T. Ohtsuki, unpublished (2003).